IOP Conf. Series: Materials Science and Engineering **1327** (2025) 012007 doi:10.1088/1757-899X/1327/1/012007

Simulation of the JT-60SA supercritical helium cooling loops during magnet integrated commissioning using Simcryogenics

François Bonne[1*] and Louis Zani[2]

[1] CEA/DSBT : Univ. Grenoble Alpes, CEA, IRIG, DSBT, 38000 Grenoble, France
[2] F4E, Broader fusion Development, 85748 Garching, Germany

[*]E-mail: francois.bonne@cea.fr

Abstract. The JT-60SA tokamak fusion experiment is under final commissioning in Naka, Japan. The magnetic confinement of this fusion facility is performed by superconducting magnets cooled to around 4.5 K. These magnets are kept in their superconducting state by a forced-flow circulation of supercritical helium (SHe) ensured by two separate cooling loops. The SHe flows through these loops by means of cryogenic circulators ensuring a flow rate of around 950 g/s, maintaining a temperature of around 4.5 K at the magnets' inlet. The first loop refrigerates the Toiroidal field (TF) magnets in parallel and, in series, their structures and the Central Soleinoid (CS) structures. The second loop refrigerates the 4 CS and the 6 Equilibrium Field (EF) magnets in parallel. A cryogenic plant capable to extract about 9 kW at 4.5 K (equivalent exergetic power) removes the heat deposited in or generated by the magnets and their structures through the SHe loops. This work presents the thermal-hydraulic model of the SHe cooling loops and the superconducting magnets circuits to predict their behavior, particularly in the event of a fast safety discharge (FSD). The modelling of the loops is made using Simcryogenics, a cryogenic simulation tool developed by CEA/DSBT. This modelling is a step towards the complete modelling of the entire cryo-magnetic system of JT-60SA, aiming to improve the control of key variables for more reliable operation. This work has been carried out within the framework of the EUROfusion Consortium, funded by the European Union via the Euratom Research and Training Programme (Grant Agreement No 101052200 — EUROfusion).

1. Introduction

The JT-60SA fusion experiment [1] is a major collaborative effort between Japan and the European Union under the Broader Approach Agreement, aimed at advancing nuclear fusion research. As an upgrade to the original JT-60 tokamak, JT-60SA features advanced superconducting coils and diagnostic systems, enabling the study of high-performance plasma scenarios critical for future fusion reactors. It is under commissioning at Naka, Japan. This paper focuses on is about its cryo-magnetic system. The magnetic system of the JT-60SA tokamak is a critical component designed to create and drive the magnetic fields configurations necessary for plasma confinement and stability. It is composed of toroidal field (TF) magnets, a central solenoid (CS), and equilibrium field (EF) magnets. There are 18 TF magnets (Nb-Ti conductor, maximum field at conductor 5.65 T), which, along with their structures, represent a mass of 420 tons. There

are 6 EF magnets (Nb-Ti conductor, peak field 6.2 T) weighing 178 tons. The CS consists of 4 modules (Nb_3Sn conductor, peak field 8.9 T) and weighs 100 tons. This study is focused on the second cryo-magnetic loop (loop 2) that ensures the circulation of supercritical helium into the EF and CS magnets. This paper is structured in 3 main sections. Section 2 presents the coldest part of the cryogenic system and the Loop 2, Section 3 details the modelling parameters of Loop 2 and Section 4 shows the simulation results. Finally, the conclusion ends the paper and outlines our future work.

2. Description of the cryo-magnetic system

The cryogenic system [2,3] consists of a warm compression station (WCS) that compresses helium from 1.05 to 15 bar. This WCS feeds a refrigeration cold box (RCB) that provides a supercritical helium flow of approximately 400 g/s at 5 K and 5 bar to an auxiliary cold box (ACB) to be used as refrigeration power. The ACB ensures the final expansion of the supercritical helium into liquid, which is stored in a large tank with a capacity of 7 m^3, serving as a thermal buffer. The liquid helium is evaporated by the heat loads from the circulators, magnets and structures through immersed heat exchangers. The resulting saturated gas flows out of the ACB and is handled by the RCB again.

2.1 Overview of the refrigeration of the magnetic system

The refrigeration of the magnetic system is organized around two supercritical helium loops, as illustrated in Figure 1. Loop 3 is not a loop from the auxiliary cold box point of view, since it takes gas directly from the process to be expanded by a valve into the bath. Loop 1 and Loop 2 work both the same way (see Figure 1). Cold circulators (CIR) generate approximately 950 g/s of supercritical helium flow cooled to the bath temperature by submerged heat exchangers (HX2 and HX4). This flow refrigerates the magnets and their structures and returns to the auxiliary cold box, where the heat absorbed from the magnet system is extracted by submerged heat exchangers

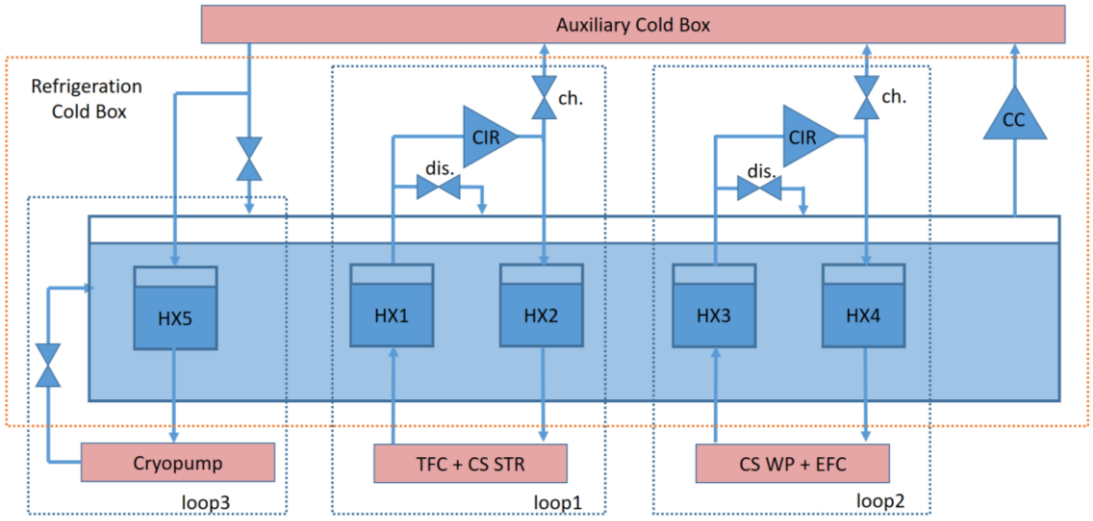

Figure 1. Auxiliary Cold Box (ACB) overview. Loop 1 and Loop 2 are dedicated to the refrigeration of magnets, with approximately 950 g/s of supercritical helium circulating through each loop via their respective circulators. Loop 3 is dedicated to the cryo-pumps. Pressure into Loop 1 and Loop 2 can be adjusted by their respective charge (ch.) and discharge (dis.) valves.

(HX1 and HX3). Details of Loop 1 modelling and simulation in the case of a fast safety discharge can be found in another publication [4]. Details about the modelling of the thermal buffer will be given in a future publication. Modelling of the cryo-magnetic part of Loop 2 is provided in the next sections.

2.2 Overwiew of Loop 2

Loop 2 ensures the refrigeration of the Central Solenoid (CS) winding packs (their structure are refrigerated by Loop 1) and the Equilibrium Field (EF) coils (EFC). Each of the four CS magnets is composed of 56 pancakes. There are six EFCs, each differing in length and pancakes organization. Figure 2 provides an overview of Loop 2. The loop operates quasi-isochorically, but the pressure can be adjusted using the charge and discharge valves. Each of the ten lines in parallel is equipped with a flowmeter, and temperature and pressure sensors at their end.

3. Modelling of Loop2

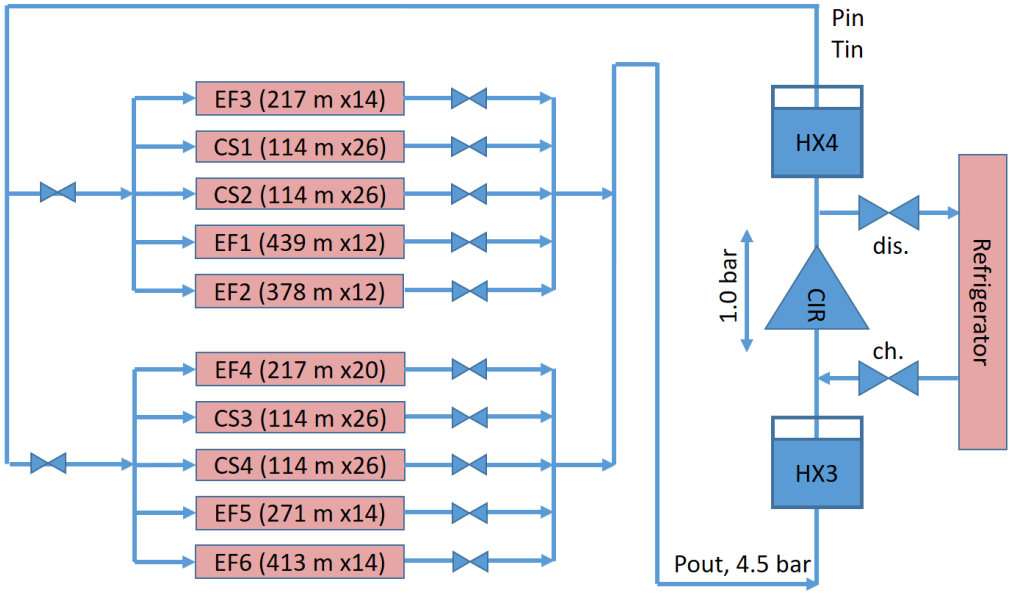

Figure 2. JT-60SA Loop 2 overview, CIR stands for circulator, ensuring around 950 g/s supercritical helium flow rate. The ch. and dis. Stand for charge and discharge valves. HX stands for heat exchanger, removing the heat generated by the circulator and that coming from the magnets. The heat exchangers are immerged into a liquid buffer helium bath at 4.3 K nominally. Each valve at the outlet of each magnet allow each helium flow to be controlled individually.

In the Loop 2, it is not possible to simplify the modelling of hydraulic circuit like in Loop 1 [4], by modelling only once the equivalent circuits in parallel. Here, the 6 EF magnets are different. The 4 CS are identical but their flowrate are different since they are individually driven by their own outlet valve. The hydraulic part of the magnets (the Cable-In-Conduit Conductor, CICC) is modelled with two pipes in parallel, respectively representing the central channel and the bundle, see Figure 3, with different characteristics, in thermal contact with each other. CICC can also exchange helium through the central channel spiral gaps all along their length [5]. The main CICCs

characteristics implemented for the modelling of Loop 2 are gathered in Table 1 and 2 while Figure 3 illustrates it. The pressure drop is calculated using the Darcy-Weisbach formula:

$$\Delta P = f \frac{L}{D_h} \frac{\rho v^2}{2}, \qquad D_h = 4.\frac{A}{W_p}$$

where ΔP is the pressure drop, f is the Darcy friction factor, L is the length of the pipe, D_h is the diameter of the pipe, ρ is the density of the fluid, v is the velocity of the fluid, A is the cross-section area, and W_p the wetted perimeter. The friction factor expected for the central channel region was originally considered to be $0.45 * Re^{-0.043}$, but was found to overestimate the pressure drop. To have a better capture of the pressure drop, we use the following available correlations [5]:

$$f_{spiral} = 0.42 * Re^{-0.1}$$
$$f_{bundle} = (0.0231 + 19.5 * Re^{-0.7953}) * void^{-0.742}$$

Table 1. Hydraulic characteristics of CICCs (1) [6,7]. SP, DP, QP and OP stand for Single, Double, Quad and Octo pancakes. The total number of pancakes of the CSs is 52 but the number of channels in parallel is 26. It is because the outlet of one pancake is connected to the inlet of one another.

	EF3	CS1	CS2	EF1	EF2	EF4	CS3	CS4	EF5	EF6
Length (m)	217	114		439	378	217	114		271	413
Channels in //	14	26		12		20	26		14	
CICC Type	EF-H	CS		EF-L		EF-H	CS		EF-L	
Organisation	7 DP	6 OP + 1 QP		12 SP		10 DP	6O P + 1 QP		7 DP	14 SP

Table 2. Main hydraulic characteristics of CICCs (2). CC stands for Central Channel. The wetted perimeter W_p can be calculated using the number of strands, their circumference and a factor 5/6.

	Inner size (mm)	Cross section (mm^2)		W_p(cm)		Nb of strands (total)	Strand diameter (mm)	Void Fraction (-)
		Bundle	CC	Bundle	CC			
EF-H	21.8 x 21.8	140		190.2		450	0.829	
EF-L	19.1 x 19.1	102	63.6	80.8	2.83	324	0.829	0.34
CS	21	96.1		79.0		324	0.82	

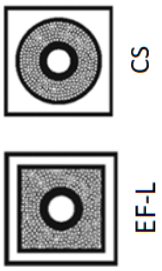

Figure 3. Geometry of the CICCs [7]

4. Comparison with experimental data

This section presents a first comparison to experimental data available from the 2021 integrated commissioning [8]. A validation in steady state is presented as well as a first dynamic scenario afterwards.

4.1 Steady State comparison

First of all, a steady state comparison is made to check the consistency of the correlations used to calculated the pressure drop of the magnets. We choose to regulate the valves in simulation in order to generate the same pressure drop as in reality and to compare the resulting flowrate in the magnets, as well as their respective resulting pressure drop. Pressures drops and flowrates are summarized in Table 3.

Table 3. Comparison of flowrates and pressure drop of the magnets with respect to experimental data. The valve pressure drop is imposed in the simulation to reproduce the one from the experimental data.

		EF3	CS1	CS2	EF1	EF2	EF4	CS3	CS4	EF5	EF6
Valve pressure drop (mbars)		699	594	380	41*	59*	619	776	525	610	223
Magnet Flowrate (g/s)	measured	45	110	155	53	66	92	116	168	60	64
	simulated	30	115	179	61	66	87	92	173	53	67
Magnet pressure difference (mbars)	measured	86	190	404	743	725	293	136	387	301	688
	simulated	65	171	385	755	753	271	114	365	280	667

* These pressure drops are not regulated since the valve is open at 100%. The valve is opened at 100% in the simulation like in the experiment

We observe that the correlations used to simulate the relationship between pressure drop and flow rate for CICC provide comparable results. The deviation between experimental and simulation could be explain with several hypothesis: the flowmeters have not been calibrated and can present a large uncertainty (even bigger when the flowrate is low comparing the nominal one); only one correlation with the same parameters is used for the 10 different CICCs and this correlation could present deviation at different flowrate and be more accurate with others. Other configurations and flow rates could be compared to ensure that the chosen correlations accurately capture the flow rate and pressure drop relationship

4.2 Dynamic scenario

The scenario involves a fast safety discharge (FSD) of Loop 1. During the Loop 1 FSD, the pressure and temperature of the thermal buffer increase, causing the pressure in Loop 2 to rise with the temperature of the thermal buffer. Since the behaviour of the thermal buffer is not modelled in this case, the experimental temperature of the bath is applied to the bath heat exchangers as an input. It can be found in [4]. The primary variables of interest in this scenario are the inlet and outlet pressures in the loop, because it is the decision variable to watch for the disconnection of the loop in case of fast safety discharge. The latter is regulated except during FSD (while the valves are at 0% opening (valve closed) on Figure 4 right) while the former pressure is the result of the pressure drop created by magnets in parallel and their respective output valves. The dynamic case show that the pressure rise due to the loop inlet temperature variation is weel captured.

5. Conclusion and future work

The supercritical helium Loops 2 of the JT60-SA cryo-magnetic system has been modelled. Simulation has been performed and the modelling validity has been assessed with experimental

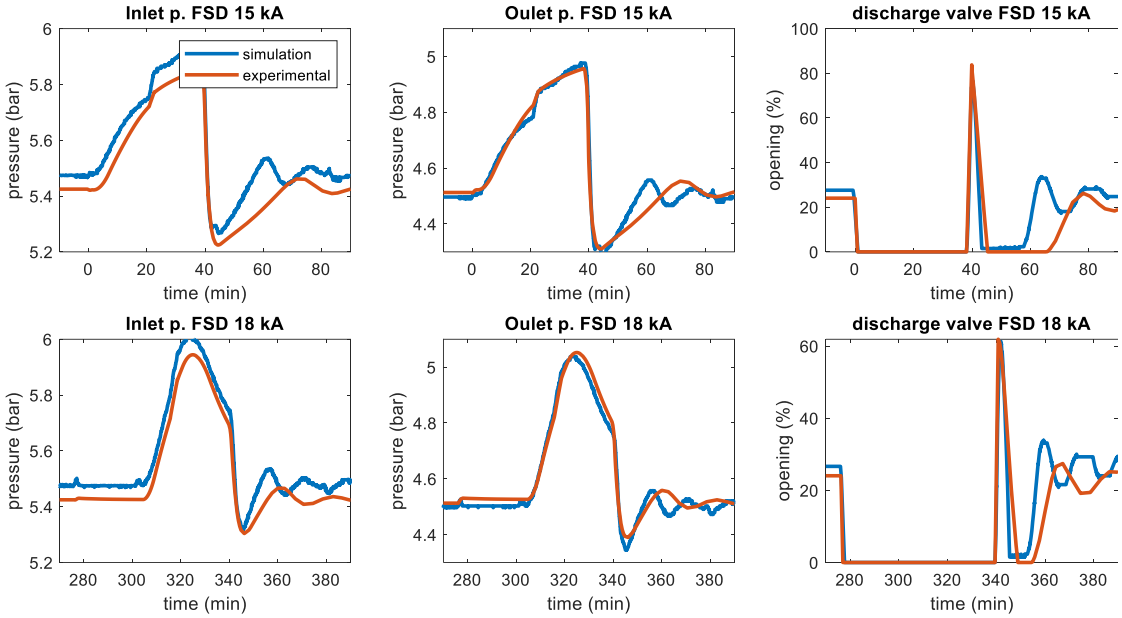

Figure 4. Inlet and outlet pressure of the Loop 2 magnets during the 15 kA and 18 kA FSD.

data. Loop 1 model has already been modelled and validated with experimental data and the thermal buffer will be the subject of another paper to come. Once gathered, it will provide a comprehensive simulation tool for analysing the cryomagnetic system. This simulator could help to predict the machine behaviour or to train operators off-line, and it could be used on-line to monitor the system. Gathering the 3 models, Loop1, Loop 2 and thermal buffer is going to be our next focus.

References

[1] Y. Kamada et al 2022 Nucl. Fusion 62 042002 doi:10.1088/1741-4326/ac10e7
[2] C. Hoa et al, “Performance of the JT-60SA cryogenic system under pulsed heat loads during acceptance tests” IOP Conference Series: Materials Science and Engineering.
[3] V. Lamaison et al. , Conceptual Design of the JT-60SA Cryogenic System”, AIP Conference Proceedings, Volume 1573, 337 (2014)
[4] F. Bonne et al. , « Simulation of the JT-60SA Supercritical Helium Toroidal Field Coil Loop During Fast Safety Discharge Using Simcryogenics. Comparison With Experimental Data and Extrapolation to Higher Currents” doi:10.1109/TASC.2024.3389943, IEEE Transactions on Applied Superconductivity
[5] S. Nicollet et al, “Dual channel cable in conduit thermohydraulics: Influence of some design parameters”. IEEE Trans. Appl. Supercond. 10, 1102– 1105. https://doi.org/10.1109/77.828425
[6] K. Yoshida *et al.*, "Conceptual Design of Superconducting Magnet System for JT-60SA," in *IEEE Transactions on Applied Superconductivity*, vol. 18, no. 2, pp. 441-446, June 2008, doi: 10.1109/TASC.2008.921970.
[7] K. Kizu *et al.*, "Conductor Design of CS and EF Coils for JT-60SA," in *IEEE Transactions on Applied Superconductivity*, vol. 18, no. 2, pp. 212-215, June 2008, doi: 10.1109/TASC.2008.920536.
[8] K. Hamada et al., "Lessons Learned From EF1 Electrical Short Incident During JT-60SA Integrated Commissioning Test," in IEEE Transactions on Applied Superconductivity, vol. 34, no. 5, pp. 1-5, Aug. 2024, Art no. 4200805,